Conference Paper

Crystal Structure of Martensite and Orientation Relationships During Thermoelastic Martensitic Transformations in Ni-Mn-Based Alloys

Elena S. Belosludtseva[1], Artemy V. Pushin[1,2], Alexey E. Svirid[1], and Vladimir G. Pushin[1,2]

[1]M.N. Miheev Institute of Metal Physics of Ural Branch of Russian Academy of Sciences (IMP UB RAS), 18 S. Kovalevskaya Street, Ekaterinburg, Russian Federation, 620108
[2]The First President of Russia B. N. Yeltsin Ural Federal University (UrFU), 19 Mira Street, Ekaterinburg, 620002

Abstract

Orientation relationships (OR’s) for the B2↔$L1_0$ thermoelastic martensitic transformations (TMT’s) in $Ni_{50}Mn_{50}$ alloy were determined by transmission and scanning electron microscopy methods, which differ from the Bain OR’s previously accepted for them. Electron microscopic studies have shown that $L1_0$ martensite has a hierarchic morphology of packets of thin plates of pairwise twinned crystals with flat boundaries of habit close to $\{110\}_{B2}$.

Keywords: thermoelastic martensitic transformation, orientation relationships, Ni-Mn, long-period crystal lattice, electron-microscopic studies.

Corresponding Author:
Elena S. Belosludtseva
ebelosludceva@mail.ru

Received: 25 February 2019
Accepted: 9 April 2019
Published: 15 April 2019

Publishing services provided by Knowledge E

© Elena S. Belosludtseva et al. This article is distributed under the terms of the Creative Commons Attribution License, which permits unrestricted use and redistribution provided that the original author and source are credited.

Selection and Peer-review under the responsibility of The Ural school-seminar of metal scientists-young researchers Conference Committee.

OPEN ACCESS

1. Introduction

The martensitic transformations in $Ni_{50}Mn_{50}$ and $Ni_{49}Mn_{51}$ alloys proceed at high temperatures, which is of particular interest for studying the structure and properties of these alloys in the transformation temperature range. In [1-11], we comprehensively investigated the structure and the physical properties of these alloys, revealed a thermoelastic mechanism of the martensitic transformations, and determined the critical temperatures of the TMTs in them (M_s = 970 K, M_f = 920 K, A_s = 970 K, A_f = 1020 K, M_s = 940 K, M_f = 930 K, A_s = 990 K, A_f = 1000 K). The high-temperature B2 → $L1_0$ phase transformations are known to occur in many binary and multicomponent intermetallic alloys based on nickel and titanium, such as Ni–Mn, Ni–Al, Ni–Mn–Al, Ni–Mn–Ga, Ni–Al–Co, Ti–Rh, Ti–Ir, Ti–Rh–Ni, and Ti–Ir–Ni, etc. [1–13]. There is reason to believe that these transformations in the alloys based on such intermetallic compounds and in other B2 nonferrous alloys (titanium nickelide, copper based alloys, ferromagnetic Heusler alloys, alloys based on alloyed manganese nickelide) also have signs of TMTs, and this fact should cause the shape memory effects in them.

2. Materials and Methods

The alloys to be studied were prepared by induction melting in a purified argon atmosphere. For homogenization, they were remelted (at least three times) and then vacuum annealed at 1173 K for up to 30 h. High-purity (99.99% purity) metals served as starting materials for the alloys. Ingots were spark cut into plates, which were then again subjected to homogenizing annealing for 6 h in the state of β (B2) phase followed by water quenching or slow cooling at a rate of ~100 K/h from 1073 or 1173 K. The temperature dependence of the electrical resistivity of the alloys (ρ(T)) were measured in the wide temperature range. The X-ray diffraction analysis by the θ/2θ method was carried out using a DRON-3M diffractometer in the Cu *K*α radiation monochromatized by a graphite single crystal. Investigations of samples were performed at room temperature after quenching and in a high-temperature vacuum chamber upon heating to the austenite state in an alloy and subsequent cooling. Transmission electron microscopy (TEM) investigations in the bright-and dark-field regimes were carried out on JEM-200 CX, Tecnai G2 30 and CM-30 transmission electron microscopes. To identify phases, we analyzed selected area electron diffraction (SAED) patterns. The structure of bulk samples and the chemical composition of a sample were analyzed with a Quanta-200 Pegasus scanning electron microscope (SEM) equipped with EDS and EBSD systems. EBSD system made possible to map crystallite misorientations in a sample. The electron-microscopic studies were performed at the Center of Collaborative Access, Institute of Metal Physics, Ural Branch, Russian Academy of Sciences.

3. Results and Discussion

Important information about the critical temperatures and physical nature of phase martensitic transitions is obtained by studies of the temperature dependences of physical properties [1-13]. For example, the method of electrical resistivity ρ(T) is often used to analyze phase structural transformations in intermetallic alloys. So, according to measurements of ρ (T) the $Ni_{50}Mn_{50}$ and $Ni_{49}Mn_{51}$ alloys studied in this work undergo two phase transitions. In the $Ni_{50}Mn_{50}$ compound, the first occurs upon cooling in the temperature range (1150 - 1100) K, and is accompanied by a decrease of ρ(T), and the second in the interval (1020 - 920) K and is accompanied by an increase of ρ(T) (Fig.1).

When alloys are heated, on the contrary, the value of ρ(T) with characteristic temperature hysteresis varies in reverse order.

In accordance with data of ρ(T), the critical temperatures of the onset (M_s, A_s) and the end (M_f, A_f) of the direct and the reverse martensitic transformations have the following values: M_s = 970 K, M_f = 920 K, A_s = 970 K, A_f = 1020 K.

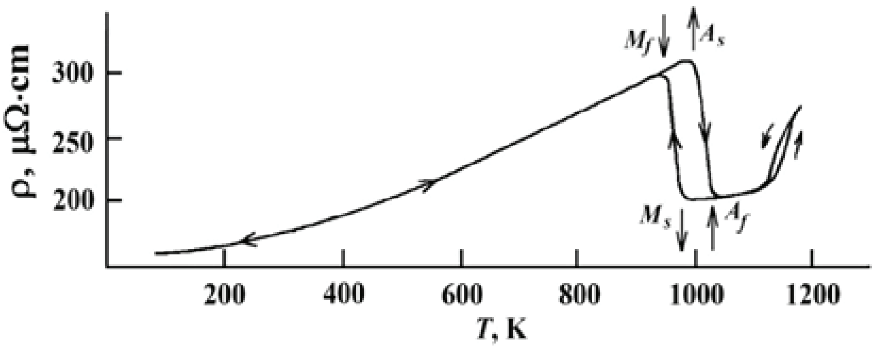

Figure 1: Temperature dependence of the electrical resistance ρ(T) in the $Ni_{50}Mn_{50}$ alloy (in the thermal measurement cycle: room temperature, RT → 1170 K → RT → boiling point of liquid nitrogen, $T_{l.n.}$ → RT).

Electron microscopic studies at room temperature determined that $Ni_{50}Mn_{50}$ and $Ni_{49}Mn_{51}$ alloys quenched from 1073 K undero the thermoelastic martensitic transformations.

Fig. 2 shows typical electron microscopic images and microelectron diffraction patterns of an equiatomic alloy after quenching. Thermoelastic martensite is a hierarchy of packages consisting of 24 variants of pairwise twinned plates with completely flat coherent interfaces between them and thin internal secondary nano-twins. The interpretation of selected electron diffraction (SAED) patterns and trace analysis shown that the lamellar crystals of the martensitic phase have a fct structure, a habit close to $(111)_{fct}$, and are twinned along the same $(110)_{B2}$ || $(111)_{fct}$ planes. Figure 2b shows a dark-field image of a quenched alloy and secondary nano twins are more clearly visible. Presence of superstructural reflections of type 001 and 110 indicates that the martensitic phase is atomic-ordered in type $L1_0$ (see Fig. 2c, and the scheme in Fig. 2 d).

In fine-grained alloys with a size of up to 5 μm, one package is usually observed (see Fig. 2a). Intergranular boundaries often have a rounded-step shape. In larger grains, many packets are joined along intragranular interpacket boundaries that separate coherently conjugated tetragonal domain inside one package (see Fig. 2b). The interpacket boundary is often not strictly crystallographic, although on average it is close to the $\{011\}_{B2}$ type plane. Parallel plates are located almost at a right angle (84° or 96°) or close to 60° to the plates of the adjacent package.

DOI 10.18502/keg.v1i1.4408

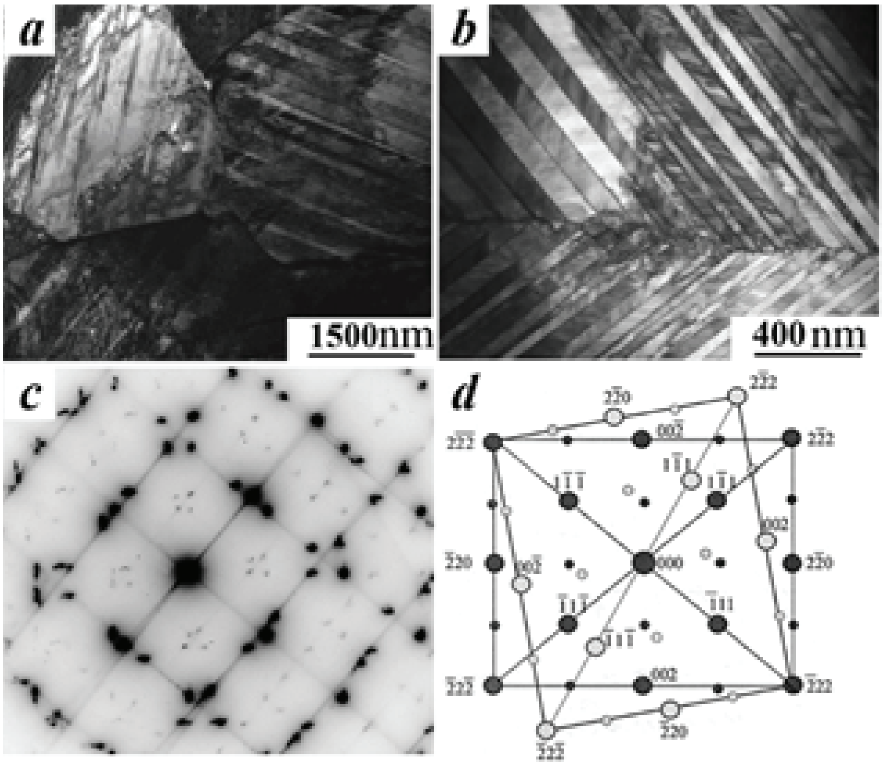

Figure 2: Typical bright (a) and dark-field (b) electron microscopic images of the structure of L1_0-martensite of the hardened $Ni_{50}Mn_{50}$ alloy at room temperature options (c), and its decryption scheme (d).

In [12, 13], it is argued that martensitic crystals are orientationally related by a ratio close to Bain's, $\{001\}_{B2}$|| $(001)_{L10}$: <110> $_{B2}$|| $[100]_{L10}$; $<\bar{1}10>$ $_{B2}$|| $[010]_{L10}$, both within a package and with crystals in adjacent packages. Crystallography TMT B2-bcc → L1_0-fct - can be represented using the Bane deformation by compressing the lattice along the $[001]_{B2}$axis and stretching along the other $[100]_{B2}$ and $[010]_{B2}$ axes to the values up to required values a and c from the L1_0 phase according to the scheme in fig. 3.

Taking into account all the obtained diffraction data, crystal geometry and size-orientation dependences, it is possible to propose another crystal-structural model of the cube-tetragon rearrangement in the TMT process in these alloys, presented in Fig. 4 [3], described by shuffling twinning shifts in planes of the type (111) $[11\bar{2}]_{L10/fct}$ || $(011)[0\bar{1}1]_{bct}$ || {110} $<1\bar{1}0>$ $_{B2}$ together with the Bain distortion B2 → L1_0, defined by the tensor:

$$\begin{pmatrix} \eta_1 & 0 & 0 \\ 0 & \eta_2 & 0 \\ 0 & 0 & \eta_3 \end{pmatrix}, \text{ where } \eta_1 = \eta_2 = \frac{a_{L10/\text{fct}}}{a_{B2}\sqrt{2}} = \frac{a_{\text{bct}}}{a_{B2}}; \eta_3 = \frac{A_{L10/\text{fct}}}{a_{B2}} = \frac{A_{\text{bct}}}{a_{B2}} \quad (1)$$

This scheme, physically more correct, provides a martensitic rearrangement of the crystal lattice by uniform atom shifting the in a direction parallel to <01$\bar{1}$ > along the {011} plane in the bct basis (or <11$\bar{2}$ > along the {111} plane in the fct basis) (Fig. 4). Twinning takes place along the same shift system. Angle β = 6,78 ° between axes a_{B2} and c_{3R}, which shown in Fig. 4, was determined experimentally at the onset temperature TMT.

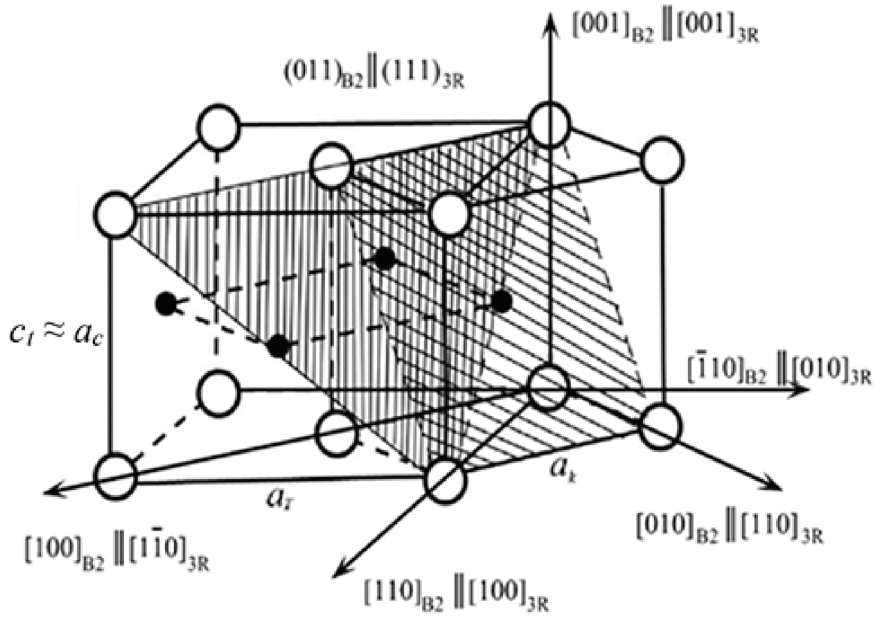

Figure 3: Model of the cubic crystal lattice of the alloy $Ni_{50}Mn_{50}$ in two crystallographic sets B2-bcc and $L1_0$-fct (3R).

In the crystal structural mechanism of TMT proposed by us for the first time, based on the analysis of selected area electron diffraction patterns were experimentally established for Ni-Mn-based alloys, in contrast to the OR used for them Bain [12, 13] the following OR, the invert OR of the Nishiyama: $(011)_{B2}$ || $(111)_{3R2M}$; $[0\bar{1}1]_{B2}$ || < $\bar{2}$11> $_{3R/2M}$ (see fig. 3).

As a result of EBSD analysis of misorientations along a straight line, a graph of the plate misorientation angle versus the starting point (Fig. 5) was plotted, the thickness of martensite plates was measured, as well as their orientation position relatively to each other. As follows from the graph, in this package, the crystallite thickness is about 0.5 μm and the angle of crystallographic misorientation between them is close to 94 ± 2 ° (86 ± 2 °), as well as according to the SAED data in TEM.

When cooled to room temperature, the angle β increases to 8 °, since the lattice parameters of the tetragonal martensite change, as shown in [2]. At the same time, adaptive thermo-elastic reorientation in packages of martensitic plates takes place in such a way that on several hierarchical levels the plate thicknesses are correlated with

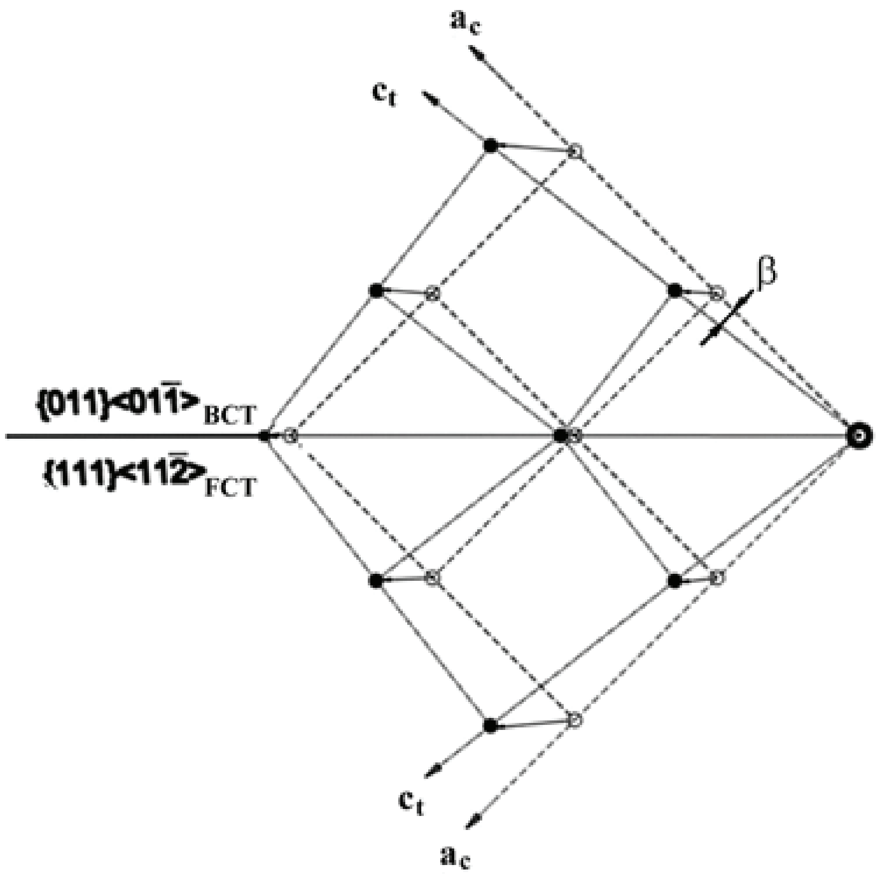

Figure 4: Scheme of shifts leading to the formation of twinned tetragonal 2M.

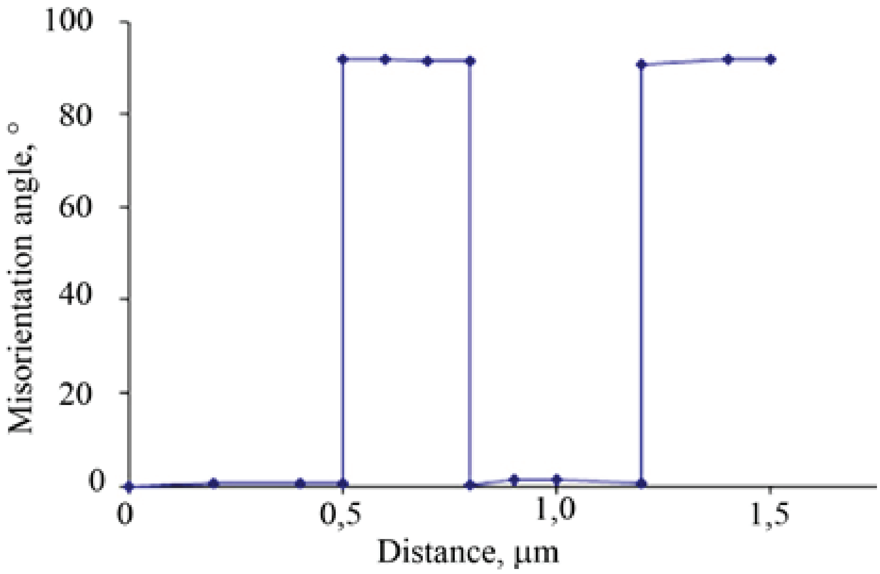

Figure 5: Disorientation of martensitic plates along a straight line.

each other on average as 1:1.3. And they are mutually self-consistent in both packages in the direction of the twinning shear, which is a characteristic property of thermoelasticity

(Fig. 6). At the same time, the nature and periodicity of zigzag shifts in the surface of the package habits are not strictly fulfilled and their “failures” take place (Fig. 6 a, b).

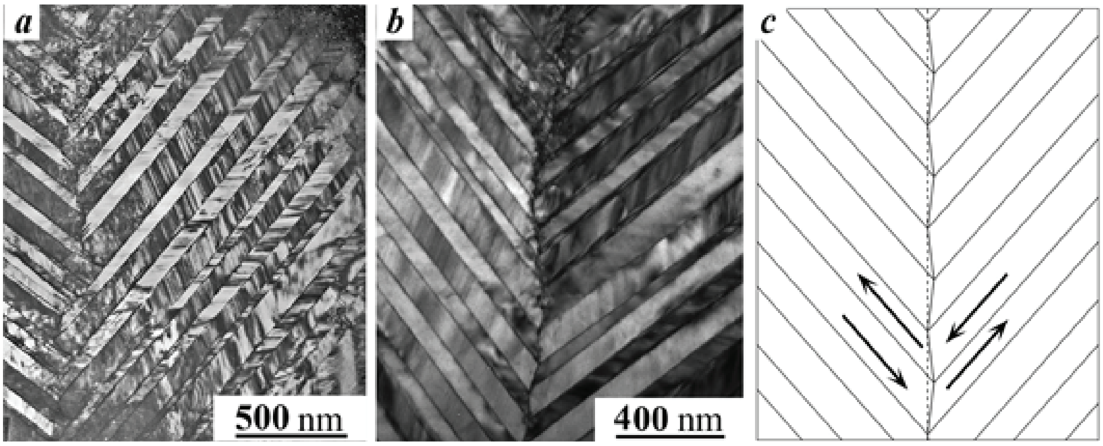

Figure 6: Images of the package structure (a, b) and plate formation scheme (c). The directions of the twinning shear are shown by arrows.

4. Summary

1. The phase compositions of the alloys under study at room temperature and the lattice parameters of austenitic and martensitic phases were established.
2. The critical temperatures of TMTs in binary alloys are determined.
3. It is shown that martensite has a predominant morphology in the form of a hierarchy of packets of thin lamellar and internally twinned crystals with flat habit boundaries $\{111\}L1_0 || \{101\}B2$.
4. Models of rearrangement of the TMT crystal lattice are constructed.
5. The crystal structure mechanism of TMTs $B2 \leftrightarrow L1_0$ (2M) for Ni-Mn alloys is proposed by a uniform shift of the atoms of the crystal lattice in the direction parallel to <01-1> along the {011} plane described in the bct basis (the {111} plane, described in the basis of the MTC-L10) and established, in contrast to the Bain orientation relations adopted for them, the relations: (011) B2|| (111) 3R / 2M; <0-11> B2 || <-211 > 3R / 2M.

Acknowledgment

The work was carried out within the framework of the state task of Russian Ministry of Education and Science (cipher ”Structure”, No. AAAA-A18-118020190116-6) and with partial support of the RFBR (project No. 18-32-00529 mol_a).

References

[1] V.G. Pushin, E.S. Belosludtseva, V.A. Kazantsev, N.I. Kourov, Features of Martensitic Transformation and Fine Structure of Intermetallic Compound $Ni_{50}Mn_{50}$, Inorganic Materials: Applied Research. 4 No. 4 (2013). 340–347.

[2] V.G. Pushin, N.N. Kuranova, E.B. Marchenkova, E.S. Belosludtseva, V.A. Kazantsev, N.I. Kourov, High-Temperature shape memory effect and the B2-$L1_0$ thermoelastic martensitic transformation in Ni-Mn intermetallics, Technical Phisics, 58 No. 6 (2013) 878 – 887

[3] V.G. Pushin, N.N. Kuranova, E.B. Marchenkova, E.S. Belosludtseva et. all, Thermoelastic Martensitic Transitions and Shape Memory Effects: Classification, Crystal and Structural Mechanisms of Transformations, Properties, Production and Application of Promising Alloys, in: V.V. Rubanik, N.N. Resnina (Eds.), Shape memory alloys: properties, technologies, opportunities, Trans. Tech. Publication, Switzeland, 2015.- 33 pp. 978-3-03835-357-7

[4] E.S. Belosludtseva, N.N. Kuranova, N.I. Kourov, V.G. Pushin, V.Yu. Stukalov, A.N. Uksusnikov, Effect of aluminum alloying on the structure, the phase composition, and the thermoelastic martensitic transformations in ternary Ni–Mn–Al alloys, Technical Physics. 60 (2015) 1000-1004.

[5] E.S. Belosludtseva, N.N. Kuranova, N.I. Kourov, V.G. Pushin, A.N. Uksusnikov, Effect of titanium alloying on the structure, the phase composition, and the thermoelastic martensitic transformations in ternary Ni—Mn—Ti alloys,Technical Physics. 69 (2015) 1330-1334.

[6] E.S. Belosludtseva, N.N. Kuranova, E.B. Marchenkova, A.G. Popov, V. G. Pushin,. Effect of gallium alloying on the structure, the phase composition, and the thermoelastic martensitic transformations in ternary Ni–Mn–Ga alloys, Technical Physics. 61 №4, (2016) 547-533.

[7] Y.V. Khlebnikova, L.Y. Egorova, D.P. Rodionov, E.S. Belosludtseva, V.A. Kazantsev, Crystallographic features of the structure of a martensite packet of the NiMn intermetallic compound, Technical Physics 61 №6 (2016) 887-897.

[8] E.S. Belosludtseva, N.N. Kuranova, E.B. Marchenkova, V.G. Pushin, Features of thermoelastic martensitic, structure and properties in ternary B2-alloys based on NiMn – NiTi, NiMn – NiAl, NiMn – NiGa, N_{i2}MnGa – Ni_3Ga quasi-binary systems, Materials Today: Proceedings. 4 (2017) 4717–4721

[9] E.S. Belosludtseva, V.G. Pushin, E.B. Marchenkova, A.E. Svirid, A.V. Pushin, Investigation of Intermetallic Alloys Based on Ni-Mn with Controlled Shape Memory Effect

Materials, Research Proceedings 9 (2018) 14-18.

[10] V.G. Pushin, E.S. Belosludtseva, E.B. Marchenkova, Multicomponent Metallic Ni–Mn-Based Alloys with Thermally, Mechanically and Magnetically Controlled Shape Memory Effects, Physics of Metals and Metallography. 119 No. 12 (2018) 1191-1195.

[11] Pre-transition phenomena and martensitic transformations, V.G. Pushin, V.V. Kondrat'ev, Physics of Metals and Metallography. 78 (5) (1994) 40-61.

[12] K. Adachi, C.M. Wayman, Transformation behavior of nearly stoichiometric Ni-Mn alloys, Met. Trans. A. 16 (1985) 1567-1579.

[13] K. Adachi, C.M. Wayman, Electron study of θ-phase martensite in Ni-Mn alloys, Met. Trans. A. 16 (1985) 1581-1597.